The NFKB Inducing Kinase Modulates Hematopoiesis During Stress

África González-Murillo, Lucía Fernández, Sara Baena, Gustavo J. Melen, Rebeca Sánchez, Carmen Sánchez-Valdepeñas, José C. Segovia, Hsiou-Chi Liou, Roland Schmid, Luís Madero, Manuel Fresno, Manuel Ramírez

The NFKB Inducing Kinase Modulates Hematopoiesis During Stress

ÁFRICA GONZÁLEZ-MURILLO,[a] LUCÍA FERNÁNDEZ,[a] SARA BAENA,[a] GUSTAVO J. MELEN,[a]
REBECA SÁNCHEZ,[b] CARMEN SÁNCHEZ-VALDEPEÑAS,[c] JOSÉ C. SEGOVIA,[b] HSIOU-CHI LIOU,[d]
ROLAND SCHMID,[e] LUÍS MADERO,[a] MANUEL FRESNO,[c] MANUEL RAMÍREZ[a]

[a]Laboratorio de Oncología, Oncohematología, FIB Hospital Universitario Niño Jesús, and Instituto de Investigación Sanitaria La Princesa, Madrid, Spain; [b]Cell Differentiation and Cytometry Unit, Hematopoietic Innovative Therapies Division, Centro de Investigaciones Energéticas, Medioambientales y Tecnológicas (CIEMAT) and Centro de Investigación Biomédica en Red de Enfermedades Raras (CIBER-ER), Madrid, Spain; [c]Cell Biology and Immunology department, Centro de Biología Molecular Severo Ochoa, Cantoblanco, Madrid, Spain; [d]Immunology, Cornell University Medical College, New York, New York, USA; [e]II, Medizinische Klinik, Technische Universität, Munich, Germany

Correspondence: Manuel Ramírez, MD, PhD, Servicio de Oncohematología, Hospital Universitario Niño Jesús. Avenida Menéndez Pelayo, 65, 28009 Madrid, Spain. Telephone: + 34915035938; Fax: + 35915035902; e-mail: manuel.ramirez@salud.madrid.org

ABSTRACT

The genetic programs that maintain hematopoiesis during steady state in physiologic conditions are different from those activated during stress. Here, we show that hematopoietic stem cells (HSCs) with deficiencies in components of the alternative NFκB pathway (the NFκB inducing kinase, NIK, and the downstream molecule NFκB2) had a defect in response to stressors such as supraphysiological doses of cytokines, chemotherapy, and hematopoietic transplantation. NIK-deficient mice had peripheral blood and bone marrow leukocyte numbers within normal ranges (except for the already reported defects in B-cell maturation); however, HSCs showed significantly slower expansion capacity in in vitro cultures compared to wild-type HSCs. This was due to a delayed cell cycle and increased apoptosis. In vivo experiments showed that NIK-deficient HSCs did not recover at the same pace as controls when challenged with myeloablative chemotherapy. Finally, NIK-deficient HSCs showed a significantly decreased competitive repopulation capacity in vivo. Using HSCs from mice deficient in one of two downstream targets of NIK, that is, either NFκB2 or c-Rel, only NFκB2 deficiency recapitulated the defects detected with NIK-deficient HSCs. Our results underscore the role of NIK and the alternative NFκB pathway for the recovery of normal levels of hematopoiesis after stress. STEM CELLS 2015;33:2825—2837

SIGNIFICANCE STATEMENT

The genetic programs that maintain hematopoiesis during steady state in physiologic conditions are different from those activated during stress. NFkB is a family of transcription factors and two main pathways have been described for NFkB activation. In this work, we show that NIK (canonical pathway) deficient hematopoietic stem cells maintain normal level of hematopoiesis under basal conditions but are functionally deficient under stress. In vivo repopulation capacity and recovery from chemotherapy, and in vitro expansion were deeply affected by NIK inactivation.

INTRODUCTION

Under homeostatic conditions, the continuous production of billions of erythrocytes, leukocytes, and platelets (PLT), and the maintenance of the immune system rely in the self-renewal and multipotential capacities of hematopoietic stem cells (HSCs). A fine regulation between self-renewal and differentiation exists. Extrinsic factors provided by the microenvironment (adhesion molecules, cytokines, and chemokines) [1, 2] as well as intrinsic factors such as transcription factors members of the Hox family [3], Bmi-1 [4], cell cycle regulators p21, p27 [5, 6], p18 [7], or the oxidative stress pathway [8–10] have been reported to modulate HSC

activities during physiological conditions. HSCs are also responsible for regenerating the hematopoietic system after several pathological and clinical situations that induce the activation of normally quiescent HSCs, and the proliferation and differentiation that ensue restores hematopoietic homeostasis [11, 12]. Less is known about the factors or mechanisms that control the response of HSCs to stressors. Deficiencies in molecular pathways involved in the response of HSCs to stress could interfere with the recovery after chemotherapy, hinder the engraftment after HSC transplantation, and also cause aplastic anemia.

NFκB is a family of transcription factors composed of homo and heterodimers of

proteins that include p105/50 (NFκB1), p100/p52 (NFκB2), p65 (Rel-A), Rel-B, and c-Rel. NFκB stimulates the expression of a panel of survival/antiapoptosis proteins and also modifies the expression of target genes of cell growth, proliferation, differentiation, immune response, and inflammation [13–15]. These proteins are located in the cytoplasm in an inactive state, but are released and translocated to the nucleus upon activation. Two main pathways have been described for NFκB activation. In the canonical pathway, IκB kinases (IKKα, IKKβ, and IKKγ) phosphorylate IκB (particularly IκBα) molecules in response to different activators (viruses, inflammatory cytokines, mitogens, and T-cell receptor signaling). IκB is also ubiquitinated and then degraded by the proteasome, releasing the NFκB transcription factors. Members of the family of TNF receptors (LTβR, CD40, BAFFR, and RANK) and some viruses (Epstein-Barr virus and human immunodeficiency virus) can activate NFκB through an alternative (noncanonical) pathway. A central component of the noncanonical pathway is the NFκB inducing kinase (NIK), a MAP kinase kinase kinase member [16, 17]. NIK was described as a serine/threonine kinase that interacted with TRAF2, activating NFκB [18]. NIK acts through IKKα [19] and stimulates the phosphorylation, ubiquitination, and processing of p100 [18, 20]. The processing of p100 generates p52 and induces nuclear translocation of RelB/p52 heterodimers. NIK can also activate c-rel transactivation activity [21].

Many groups have studied the role of NIK and the noncanonical pathway in the immune system. Inactivation or deficits in this pathway negatively affected the numbers and functions of B and T lymphocytes [22, 23], and the structure of lymphoid organs [24]. Deficiencies in NIK activity resulted in impaired models of immune diseases such as graft versus host disease (GVHD) [21, 25], experimental autoimmune encephalomyelitis (EAE) [26], and arthritis [27]. Conversely, deregulated (constitutively activated) activation of the noncanonical NFκB pathway has been described in human diseases and contributes to the development of lymphoid malignancies [28–31], multiple myeloma [32], and solid tumors [33–36]. However, there are few studies on the role of NIK or the alternative pathway in HSCs function [37]. We previously described that GVHD did not occur when donor cells had an inactive NIK protein, due to increased apoptosis of T lymphocytes [21]. In this article, we have focused on the role of NIK in another major item in stem cell transplantation, that is, hematopoietic regeneration. We found that NIK deficiency confers a proliferative disadvantage and increased apoptosis in HSCs in the transplantation context, and confirmed these findings in different stressful conditions. All these defects were recapitulated using HSCs from an NFκB2-deficient mouse. Our results underscore a role for NIK and the alternative NFκB pathway in HSCs function after stressful situations.

MATERIALS AND METHODS

Mice and Irradiation Procedures

NIK-deficient *aly/aly* mice (NIK$^{aly/aly}$) [22], *NFkB2*$-/-$ [38], and *cRel*$-/-$ mice [39], all in the C57BL6 background, have been previously described. C57BL6 (WT, CD45.2), P3B (CD45.1), and P3D2F1 (CD45.1/CD45.2) mice were used as donors and recipients in experiments of bone marrow (BM) transplant. Experimental procedures were performed at CIE-

MAT Laboratory Animals Facility (registration number 28079-21 A) and Centro de Biología Molecular Severo Ochoa (registration number 28079-19A). Mice aged 8–12 weeks old were used. P3B recipient mice (CD45.1 females) were irradiated with two doses of 5.5 Gy spaced 24 hours. Animals were irradiated with Philips MG 324 X-ray equipment (Philips, Hamburg, Germany, http://www.healthcare.philips.com). All experimental procedures were carried out according to European and Spanish laws and regulations (European convention ETS 1 2 3, about the use and protection of vertebrate mammals used in experimentation and other scientific purposes; Spanish RD 1201/2005, about the protection and use of animals in scientific research). The Animal Experimentation Ethical Committee of the CIEMAT approved procedures, according to all external and internal biosafety and bioethics guidelines.

Flow Cytometry

Peripheral blood (PB) or BM cells were first incubated with monoclonal antibodies for 30 minutes at 4°C, and then lysed (QuickLysis, Cytognos, Salamanca (Spain), http://www.cytognos.com/) for 20 minutes at room temperature to eliminate erythrocytes. Flow cytometry acquisition and analysis were performed on a FACS Canto II cytometer (BD Bioscience, Franklin Lakes, NJ, http://www.bdbiosciences.com/eu/home) using the FACS Diva software.

To analyze engraftment kinetics, PB or BM cells were stained with CD45.2-FITC (BD Bioscience, Franklin Lakes, NJ, http://www.bdbiosciences.com/eu/home) or CD45.2-APC (Immunostep, Salamanca, Spain. http://immunostep.com/) antibodies. To analyze lineage differentiation, cells were stained with CD3-PECy7 (BD Bioscience, Franklin Lakes, NJ, http://www.bdbiosciences.com/eu/home), B220-PE (BD Bioscience, Franklin Lakes, NJ, http://www.bdbiosciences.com/eu/home), and GR1-PE (Biolegend, San Diego, CA, http://www.biolegend.com). For phenotype analysis, hematopoietic cells were harvested from BM, lysed, and stained with a cocktail of differentiation markers APC- or FITC-conjugated (BD Bioscience, Franklin Lakes, NJ, http://www.bdbiosciences.com/eu/home). Monoclonal antibodies used for flow cytometry analysis of immature progenitors were: CD117/c-kit APCCy7 (Biolegend), Sca1 PE-Cy7 (BD Bioscience, Franklin Lakes, NJ, http://www.bdbiosciences.com/eu/home), CD48 PE-Cy7 (BD Bioscience, Franklin Lakes, NJ, http://www.bdbiosciences.com/eu/home), CD244.2 PE (BD Bioscience, Franklin Lakes, NJ, http://www.bdbiosciences.com/eu/home), CD150 FITC (BD Bioscience, Franklin Lakes, NJ, http://www.bdbiosciences.com/eu/home), CD34-FITC (BD Bioscience, Franklin Lakes, NJ, http://www.bdbiosciences.com/eu/home), FLK2/CD135-PE (BD Bioscience, Franklin Lakes, NJ, http://www.bdbiosciences.com/eu/home), Sca1-APC-Cy7 (Biolegend, San Diego, CA, http://www.biolegend.com), CD150-APC (Biolegend, San Diego, CA, http://www.biolegend.com), and CKit/CD117-PECy7 (Biolegend, San Diego, CA, http://www.biolegend.com).

For cell cycle analysis, BM or Lin$^-$Sca1$^+$cKit$^+$ (LSK) sorted cells were stained in cold Hoechst staining buffer with 5 μg/ml Hoechst 33342 at 37°C, 45 minutes. Pyronin Y was added at a final concentration of 0.5 μg/ml and the cells were further incubated 45 minutes [6]. Then cells were spun down (4°C), stained for surface markers, and resuspended in ice-cold Hoechst staining buffer.

For LSK sorting, we used a Beckman Coulter EPICS ALTRA Cell Sorter (Beckman Coulter, Fullerton, CA. www.beckman

coulter.com). Apoptotic/dead cells were identified by annexin-V (PE or APC, BD)/7-amino-actinomycin D (or DAPI).

Competitive Repopulation Assay and Serial Transplantation

For lineage negative (Lin−) purification, BM cells were obtained from the femurs and tibias of donor mice and depleted of lineage-positive cells with the Lineage Cell Depletion Kit (Miltenyi Biotech, Bergisch Gladbach, Germany, http://www.miltenyibiotec.com/) following the manufacturer's recommendations. For competitive repopulation assay Lin− cells (or total BM) from NIK$^{aly/aly}$, NFkB2$^{−/−}$, or cRel$^{−/−}$ (CD45.2) male mice were mixed at 1:1 or 1:3 ratios with competitor P3B (CD45.1) cells. A total of 10^7 total BM cells or 2×10^5 Lin− cells were transplanted into lethally irradiated P3D2F1 or P3B female. Engraftment kinetics and lineage differentiation markers in PB were analyzed monthly by flow cytometry. LSK phenotype of CD45.2 population was analyzed in BM of transplanted mice at 5 months post-transplantation. At this time, BM cells from primary recipients were obtained, and 10^7 chimeric total BM cells were transplanted into lethally irradiated P3B female in serial transplant assays. Engraftment kinetics was analyzed at PB 1 and 2 months after secondary transplants. DNA was extracted from PB using DNAeasy Mini Kit (Qiagen, Hilden, Germany. https://www.qiagen.com), and exogenous reconstitution was determined by Q-PCR analyses, conducted in a 7500 Real-Time PCR System (Life Technologies, Applied Biosystem. Foster City, CA, www.lifetechnologies.com), and using primers and a probe for the SRY gene, specific to the Y chromosome as described before [40].

Homing Assay

A total of 5×10^6 BM cells from NIK$^{aly/aly}$ or WT were transplanted into lethally irradiated female P3B mice. After 16 hours, mice were sacrificed and CD45.2 engraftment was analyzed by flow cytometry of BM.

BM Transplantation and 5-Fluorouracil Treatment

5-Fluorouracil (5-FU, Sigma Chemicals, St. Louis, MO, http://www.sigmaaldrich.com/) was administered at a dose of 150 mg/kg b.wt. through tail vein in mice transplanted with NIK$^{aly/aly}$, NFkB2$^{−/−}$, or WT BM cells, 2 months after BM transplantation. PB cell counts (Beckman Coulter, Fullerton, CA, www.beckmancoulter.com) and BM cellularity were determined at the indicated time points. Percentage of LSK cells, apoptosis, and cell cycle status were analyzed from BM cells at 2 and 6 days post-treatment.

Western Blot Analysis

Western blot analyses were performed using whole cell lysate prepared from BM from 5-FU treated mice prepared with RIPA buffer (Sigma Chemicals, St. Louis, MO, http://www.sigmaaldrich.com/). Samples were separated on 10% polyacrylamide gels and transferred to nitrocellulose membranes for antibody detection. All membrane-blocking steps and antibody dilutions were performed with 5% Bovine Serum Albumin (BSA) in Tris Buffered Saline (TBS) containing 0.1% Tween 20 (TBS-T), and washing steps performed with TBS-T. The primary antibodies used were anti P100 (4882, Cell Signaling Technology, Danvers, Massachusetts, http://www.cellsignal.com/) and anti-Actin (I-19) (SC16 16 Santa Cruz Biotechnology, Inc.Dallas, TX, http://www.scbt.com). After incubating with HRP-coupled secondary antibodies, Western blots were visualized by Immun-Star WesternC (Bio-Rad Laboratories, S.A., Alcobendas, Spain, http://www.bio-rad.com/).

In Vitro Cultures

Clonogenic assays were done to determine granulocyte-macrophage colony-forming units (CFU). Total BM cells were seeded in MethoCult GF M3534 culture media (Stem Cell Technologies, Vancouver, BC, Canada, http://www.stemcell.com/) and cultured at 37°C in 5% CO_2 and fully humidified air. Colonies were scored after 7 days of culture.

10^5 Lin− purified cells or 10^4 freshly sorted LSK cells from NIK$^{aly/aly}$ and WT mice BM were cultured in Iscove's Modified Dulbecco's Medium (IMDM) (Gibco Laboratories, Grand Island, NY, www.lifetechnologies.com) medium with 20% Fetal Bovine Serum (FBS) (Lonza, Basel, Switzerland, http://www.lonza.com), Glutamine/Pen-strepto (Gibco Laboratories, Grand Island, NY, www.lifetechnologies.com), 100 ng/ml hIL11 (Miltenyi Biotech, Bergisch Gladbach, Germany, http://www.miltenyibiotec.com/), and 100 ng/ml mSCF (Miltenyi Biotech, Bergisch Gladbach, Germany, http://www.miltenyibiotec.com/) [41]. Total cells were counted weekly, and diluted to the initial concentration.

For proliferation assay, Lin− cells were stained with Carboxyfluorescein succinimidyl ester (CFSE) (Molecular Probes. Eugene, OR, www.lifetechnologies.com) following manufacturer's instructions. Labeled cells were cultured in supplemented medium and CFSE dilution was analyzed daily by flow cytometry. Apoptosis was also analyzed in these cultures as explained before.

Gene Expression Microarray

Total RNA was isolated from freshly sorted LSK population of WT and NIK$^{aly/aly}$ mice using TRIzol reagent (Invitrogen, Carlsbad, California, www.lifetechnologies.com) and its quality checked in the Agilent 2100 Bioanalyzer platform (Agilent Technologies, Santa Clara, CA, http://www.chem.agilent.com/). To produce Cy3-labeled cRNA, the RNA samples were amplified (using a linear T7-based amplification step) and labeled using the Agilent Low Input Quick-Amp Labeling kit (Agilent Technologies, Santa Clara, CA, http://www.chem.agilent.com/). The hybridization procedure was performed according to the Agilent 60-mer oligo microarray processing protocol using the Agilent Gene Expression Kit to a Agilent Whole Mouse Genome Oligo Microarrays 8x60K. We analyzed three samples as independent triplicates for NIK$^{aly/aly}$ and for WT. Each LSK sample was the pool of three to four mice. Microarray analysis was performed with Agilent Whole Mouse Genome Oligo Microarrays. Student's test was applied on the normalized log 2-ratio intensity data to distinguish expression differences between WT and NIK$^{aly/aly}$ sample groups. Candidate genes were required to have an expression difference of at least 1.5-fold, with p-value less than or equal to .05. Search for transcription factor binding sites was performed with MatInspector (Genomatix, München, Germany, www.genomatix.de). Pathway analysis was carried out on the Ingenuity Pathway Analysis (IPA) platform (Qiagen, Hilden, Germany, https://www.qiagen.com). Microarray data are available under GSE63702 at http://www.ncbi.nlm.nih.gov/geo/.

Statistics

All statistical analyses were performed using Stata/IC 11.0 (StataCorp LP, College Station, TX, http://www.stata.com/).

The nonparametric Wilcoxon rank-sum test was used to compare quantitative variables. Results were considered statistically significant with $p < .05$. All graphics present the mean $\pm$ SE.

RESULTS

Hematopoiesis of NIK-Deficient *aly/aly* Mice Is Normal Under Steady-State Conditions

Basal hematopoiesis was studied in PB and BM of adult NIK*aly/aly* and WT mice. Apart from the already reported defects in B-cell maturation [22–24], NIK*aly/aly* mice did not present major disturbances in PB leukocyte numbers. The cellularity of white blood cells (WBC), PLT, and red blood cells was not significantly different comparing mutant and wild-type mice. Cellularity and lineages in BM were also within normal ranges (Supporting Information Fig. S1A).

To study the committed compartment, we next performed clonogenic assays from BM cells. NIK*aly/aly* mice presented numbers of CFU colonies that were not significantly different than those of controls (Fig. 1A).

To study the stem cell compartment, we analyzed BM using multiparametric flow cytometry. Several populations containing hematopoietic stem and progenitor cells, such as LSK [42, 43], LT-HSC (LSK CD135-CD150+CD34−) [44], ST-HSC (LSK CD135−CD150+CD34+), MPP (LSKCD135+), or the SLAM (Lin^neg^CD150+CD48−) HSCs [45, 46] were studied (Fig. 1B and Supporting Information Fig. S1B). Although values tended to be lower in LSK, LT-HSC, and SLAM populations (not in ST-HSC and MPP), there were no statistically significant differences in any populations between NIK*aly/aly* mice and those in WT. Proportions of Sca1+ cells in NIK*aly/aly* BM were lower than in WT, reflecting the deficit in B-cell progenitors [47]. In addition to the HSC phenotype, we found similar distribution of cells in the G_0, G_1, and $S/G_2/M$ phases of the cell cycle in LSK and SLAM HSCs from NIK*aly/aly* BM compared with control mice, in the steady state (Fig. 1C). All the above indicated that NIK inactivation (*aly* mutation) did not affect mature PB lineages (except for B-cells), progenitor compartment, absolute numbers and quiescence of HSC subpopulations in steady-state hematopoiesis.

NIK*aly/aly* Mice Show a Defect in Reconstitution Ability

We next studied the effects of NIK deficiency in situations of stress. Since recovery of the hematopoietic system after BM transplantation is the most stressful condition for HSCs, we performed a serial transplantation assay using cells from NIK*aly/aly* and WT BM cells. We first transplanted CD45.2 cells into lethally irradiated P3B mice (10^7 cells per recipient animal). NIK*aly/aly* and WT HSCs similarly and completely reconstituted the hematopoiesis of primary recipients in a WT environment (Fig. 2A). Two months after this first transplant, CD45.2 donor-derived cells were recovered from BM (with similar engraftment values than PB, data not shown), mixed at a 3:1 ratio with fresh competitor CD45.1 cells, and transplanted into lethally irradiated mice (P3D2F1, CD45.1/CD45.2) (Fig. 2A). Short- and long-term hematopoiesis were analyzed monthly in PB. We found that NIK*aly/aly* PB chimerism was significantly lower than WT at 1 month post-transplant (mpt) (Fig. 2A and Supporting Information Fig. S2A), and decreased

over time in secondary recipients (Fig. 2A and Supporting Information Fig. S2A). These data indicate that NIK deficiency promotes HSC depletion during serial transplantation.

To further evaluate the self-renewal capacity of NIK*aly/aly* and WT HSC in vivo, we performed a competitive repopulating assay using linage-depleted BM cells (Lin− population), where Lin− CD45.2+ cells (NIK*aly/aly* or WT) were mixed at a 1:1 ratio with competitor Lin− CD45.1+ (P3B mice) and transplanted into lethally irradiated (CD45.1, P3B male) mice (Fig. 2B). Endogenous hematopoiesis analyzed was consistently lower than 10% (data not shown) [40]. The level of engraftment of NIK*aly/aly*-derived cells was analyzed monthly in PB. Engraftment level at 1 mpt (short-term reconstitution ability) of NIK*aly/aly* CD45.2+ cells was comparable to that of WT CD45.2+ cells but this contribution decreased in the long-term (Fig. 2B). The values of NIK*aly/aly* CD45.2+ were significantly lower than the WT at 5 mpt, in PB (Fig. 2B) and BM (Fig. 2C). Further analysis of BM in recipient mice showed that NIK deficiency resulted in a significant decrease of absolute numbers of LSK 5 mpt (Fig. 2D), suggesting that NIK*aly/aly* HSCs have diminished self-renewal ability.

We also analyzed lineage differentiation in PB of recipients, and found that both NIK*aly/aly* and WT HSCs repopulated a multilineage hematopoiesis upon transplantation (Supporting Information Fig. S2B). A significant difference was observed in the contribution of myeloid versus B lymphocytes compartment in the reconstitution of NIK*aly/aly* and WT hematopoiesis (Supporting Information Fig. S2B).

To further confirm a defect in reconstitution ability, chimeric BM cells were retransplanted into secondary recipient mice 5 mpt. The low engraftment values of CD45.2 NIK*aly/aly* were maintained at minimal percentages (Fig. 2E). The analyses of PB of secondary recipients confirmed the repopulation capacity defect of the HSCs with a NIK inactivated protein.

NIK*aly/aly* HSCs Show a Intact Homing Ability

To rule out whether the defect in reconstitution ability showed by NIK*aly/aly* HSC was secondary to a defect in homing, we transplanted total BM from NIK*aly/aly* mice or WT into lethally irradiated P3B mice and analyzed marrow and spleen 16 hours after transplant. The absolute numbers of donor LSK CD45.2+ cells were similar comparing NIK*aly/aly* versus WT (Fig. 3). This data suggested that NIK activity is dispensable for the efficient homing of HSCs in the BM. Thus, our results clearly indicated a defective repopulation ability of NIK*aly/aly* HSCs, not due to a defect in their homing ability.

NIK*aly/aly* HSCs Show a Delayed Hematopoietic Recovery After Myeloablative Chemotherapy

To further evaluate the influence of NIK*aly/aly* mutation on the reconstitution capacity of HSCs under hematopoietic stress, we analyzed HSC at different points following myeloablative chemotherapy. 5-FU is a known myeloablative agent used in cancer therapy. In the hematopoietic system, 5-FU kills cycling cells, including progenitors, and induces the cycling of more primitive HSCs. To confirm that 5-FU therapy activated the NFκB alternative pathway in hematopoiesis, we treated NIK*aly/aly* and WT mice with 5-FU and did Western blot on extracts from BM cells. A significant reduction in the expression of p52 was found in aly/aly mice, while p100 was detected at comparable levels compared to control [24] (Supporting Information Fig. S3).
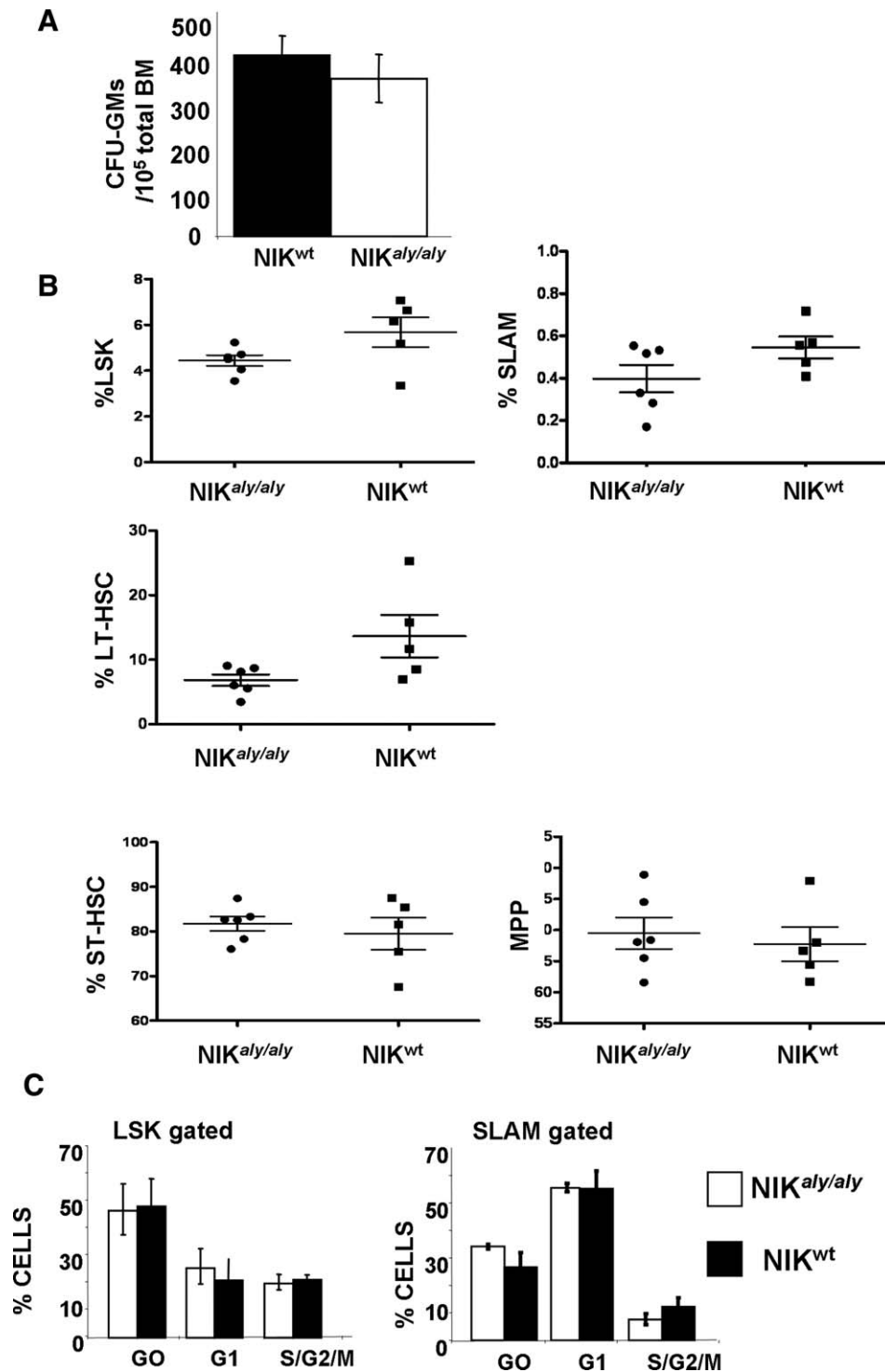
Figure 1. Dispensable role of NIK in steady-state hematopoiesis. **(A)**: Clonogenic assays cultured in semisolid medium to study the myeloid progenitor compartment in basal conditions and after 7 days of cytokines exposure. **(B)**: Stem cell compartment. Bone marrow (BM) samples were analyzed by flow cytometry. LSK (Lin−Sca1+cKit+), SLAM (Lin−CD150+CD48−), LT-HSC (LSKCD135−CD150+CD34−), ST-HSC (LSK CD135−CD34+), and MPP (LSK CD135+) HSCs were studied (NIK$^{aly/aly}$ $n = 6$; WT $n = 5$). **(C)**: Cell-cycle status of HSCs by analyzing RNA and DNA content. Distribution of cells in the G0, G1, and S/G2/M phases of cell cycle in LSK and SLAM HSCs from NIK$^{aly/aly}$ ($n = 5$) BM compared with control mice ($n = 10$). Abbreviations: CFU-GM, granulocyte-macrophage colony-forming unit; HSC, hematopoietic stem cell; LSK, Lin$^-$Sca1$^+$cKit$^+$; NIK, NFκB inducing kinase.

To exclude the potential effects of 5-FU on nonhematopoietic tissues, we first transplanted NIK$^{aly/aly}$ or WT BM cells into lethally irradiated CD45.1 mice. Two months later, we confirmed total engraftment of donor cells [48]. A single dose of 5-FU was injected and WBC counts were obtained at 4, 10, 15, and 32 days post-treatment (dpt). PB counts in WT
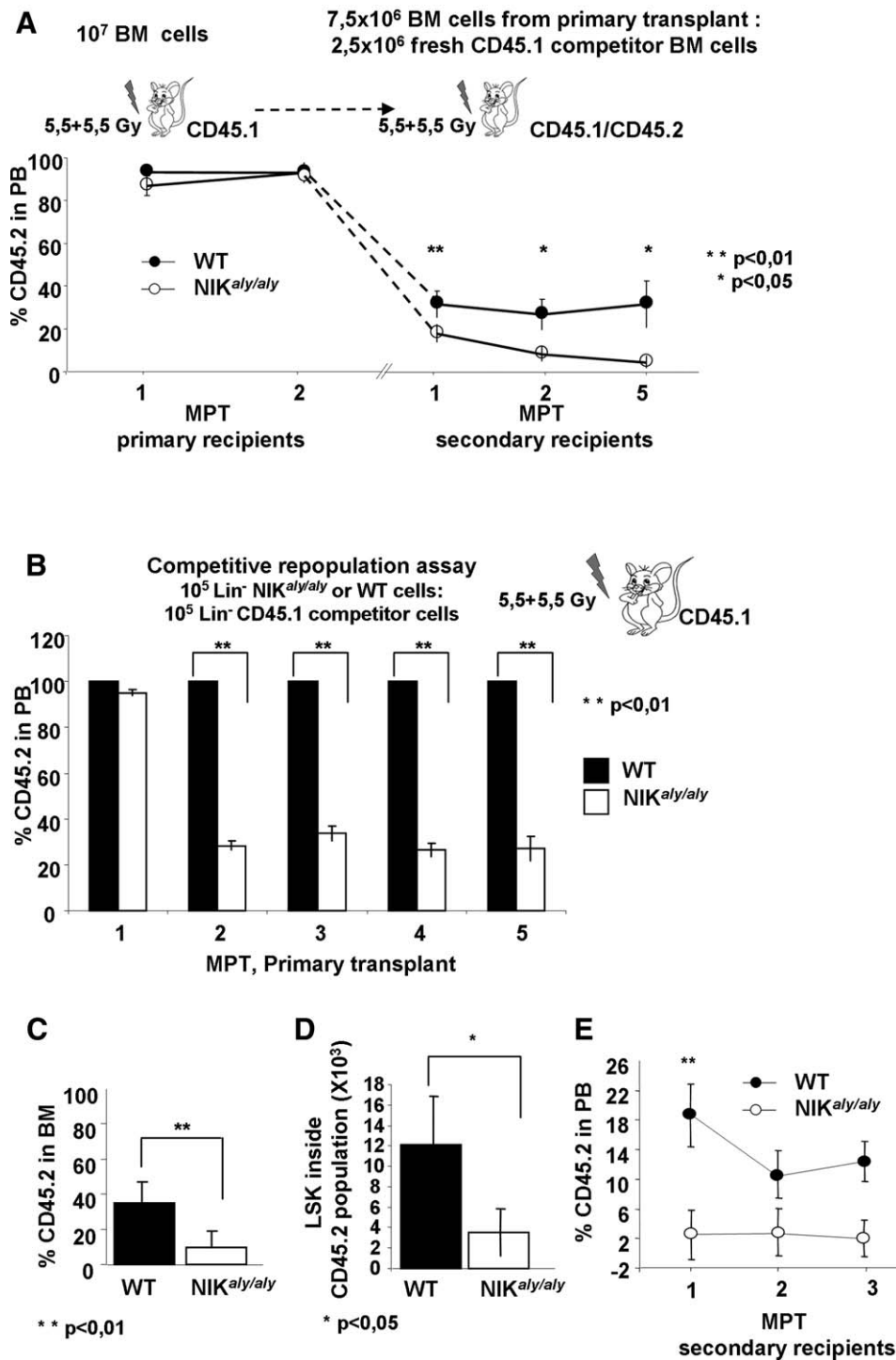
Figure 2. Impaired responses of hematopoietic stem cells NIK$^{aly/aly}$ to stressors. **(A)**: Two-step transplantation assay. After total reconstitution of primary recipients with NIK$^{aly/aly}$ or WT cells, secondary transplant was performed with 7.5×10^6 cells of total BM from primary recipients mixed with 2.5×10^6 fresh competitor and kinetics of CD45.2 population was analyzed at 1, 2, and 5 mpt in PB of transplanted mice ($n = 5$ per group). **(B)**: Competitive repopulation assays. Engraftment kinetics of CD45.2 population in PB of lethally irradiated mice transplanted with a mix of linage negative (Lin$^-$) CD45.2$^+$ cells from BM of female NIK$^{aly/aly}$ or WT mice with competitor ($n = 10$ per group, two independent experiments). **, $p < .01$. The results are normalized to the engraftment levels of WT cells ($n = 5$ per group) **, $p < .01$. **(C)**: Engraftment levels in BM of primary recipients at 5 months post-transplant **, $p < .01$. **(D)**: Absolute numbers of CD45.2 + LSK (percentage of Sca1+cKit + cells within the Lin− population) cells in BM of primary recipients at 5 months post-transplant. *, $p < .05$. **(E)**: Engraftment kinetics of CD45.2 population in PB of secondary recipients. Abbreviations: BM, bone marrow; LSK, Lin$^-$Sca1$^+$cKit$^+$; NIK, NFκB inducing kinase.
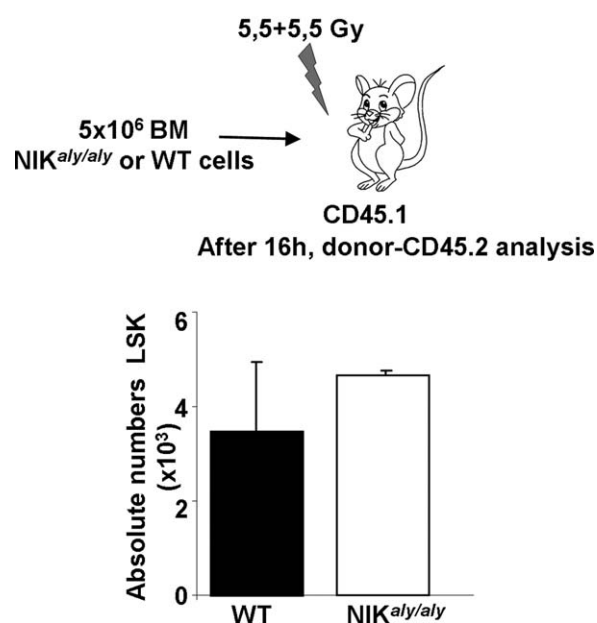
Figure 3. Homing ability of hematopoietic stem cells was not affected by the NIK$^{aly/aly}$ mutation. Absolute numbers of CD45.2 + LSK (percentage of Sca1+cKit + cells within the Lin− population) cells in BM of lethally irradiated P3B mice analyzed 16 hours after transplant ($n = 5$ per group). Abbreviations: BM, bone marrow; LSK, Lin−Sca1$^+$cKit$^+$; NIK, NFκB inducing kinase.

chimera at 4 dpt were slightly lower (but not significant) compared to those in NIK$^{aly/aly}$ chimera (Fig. 4A). The recovery of the PB leukopenia was delayed in NIK$^{aly/aly}$ chimeric mice compared to controls (at 15 and 30 dpt) (Fig. 4A), indicating that NIK plays an essential role in HSC proliferation after a stressor such as myelotoxic chemotherapy.

The absolute numbers of LSK cells in BM were no different between NIK$^{aly/aly}$ and WT mice. Significantly higher percentages of LSK NIK$^{aly/aly}$ were detected 6 days post-treatment compared to those at day 2 (Fig. 4B). To further study the response of HSC to 5-FU, we performed apoptosis and cell cycle analysis of LSK at days 2 and 6. Proportions of quiescent cells (G0) diminished over the 6 days period, and were always significantly higher in NIK$^{aly/aly}$ versus WT LSK. On the contrary, percentages of cycling LSK were significantly lower among NIK$^{aly/aly}$ versus WT at days 2 (S phase) and 6 (G2/M). The analysis of apoptosis showed a significant decreased in the proportion of living cells at days 2 and 6 among NIK$^{aly/aly}$ LSK cells (Fig. 4D). These data suggested that NIK deficiency compromised the HSC reconstitution ability after myeloablative chemotherapy, due to a delayed cell cycle progression and an elevated apoptosis rate. Together with the competitive repopulation experiments, these results show that HSCs need a fully active NIK protein to cope with stressful conditions in vivo.

Aly/aly Progenitor Cells Have a Defective Expansion Capacity Due to an Impaired Proliferation and Increased Apoptosis During Stress

We also studied the effect of supraphysiological levels of cytokines that drive hematopoietic cells into expansion in vitro. We set up in vitro experiments to assess the proliferative capacity of hematopoietic cells. Liquid cultures of Lin− cells

from NIK$^{aly/aly}$ or WT mice were maintained during 14 days. Total numbers of cells were determined weekly and we observed a significant impairment in the expansion capacity of Lin− cells from NIK$^{aly/aly}$ versus WT mice (Fig. 5A). These results were confirmed with a more homogeneous starting HSC population. Ten thousand sorted LSK cells were placed in liquid cultures and cells were counted weekly. After 14 days, a significant decrease in the fold expansion was observed in NIK$^{aly/aly}$ HSC compared with WT HSC cells (Fig. 5B). These data suggested that NIK$^{aly/aly}$ have a defective proliferative capacity in the HSC compartment.

One possible explanation for this may be a defective proliferation of NIK$^{aly/aly}$ hematopoietic cells compared to controls. To test this hypothesis, Lin− BM cells were labeled with CFSE and dye dilution was analyzed as a means to evaluate rounds of cell division. A marked delayed in the CFSE dilution was observed in NIK$^{aly/aly}$ cells compared with WT ones. At day 2, approximately more than 70% of WT cells had undergone three or more cell divisions, while only 18% NIK$^{aly/aly}$ cells had reached three rounds of cell division (Fig. 5C). This result indicated that the expansion defect in Lin− cells from NIK$^{aly/aly}$ mice was due in part to a defect in the proliferation capacity. This result is consistent with the delayed recovery observed after 5-FU treatment in vivo by accumulation on G0 phase and with the severe proliferative disadvantage observed in competitive repopulating assays.

An increased rate of apoptosis of proliferating NIK$^{aly/aly}$ hematopoietic cells could also account for the differences in the final total numbers. We analyzed cell viability to rule out that an increased apoptotic ratio could explain the expansion defect after exposure to cytokines. We found that NIK$^{aly/aly}$ and WT hematopoietic cells differed in the proportions of apoptotic cells in culture. Both at days 2 and 5 after culture initiation, NIK$^{aly/aly}$ BM cells presented higher rates of apoptosis compared with WT hematopoietic cells (Fig. 5C). The differences at day 2 were statistically significant. Similarly as 5-FU treated BM, these results indicated that NIK plays an important role for maintaining viability of hematopoietic cells after a proliferative stress.

The NIK-NFκB2 Pathway Controls HSCs During Stress Hematopoiesis

Since NIK may signal through p100/p52 [18] and cRel [49], we further investigated which of those pathways were involved in the deficiencies found with the NIK$^{aly/aly}$ HSCs. For this, we used NFκB2$^{−/−}$ [38] and cRel$^{−/−}$ [39] mice and repeated the experiments discussed above. The results obtained when using NFκB2$^{−/−}$ HSCs were comparable to those described with NIK$^{aly/aly}$ cells in similar experimental conditions. In competitive repopulation assays, the levels of chimerism (donor CD45.2 cells) in PB of mice transplanted with cRel$^{−/−}$ HSCs were not inferior to those of mice transplanted with WT HSCs (Fig. 6A), while mice transplanted with NFκB2$^{−/−}$ HSCs showed significantly lower levels than control (Fig. 6B). Furthermore, the levels of NFκB2$^{−/−}$ engraftment decreased from 1 mpt to the end of the experiment (25% at 1 mpt to 10% at 5 mpt) (Fig. 6B). The differentiation into B and T lymphoid and myeloid lineages was normal in PB cRel$^{−/−}$ engraftment but not in NFκB2$^{−/−}$ (CD45.2) (Supporting Information Fig. S4). These results suggest that defects in the NIK-p100/p52 pathway but not in NIK-cRel pathway result in HSC dysfunction under proliferative stress conditions. Proliferation defect of NFκB2$^{−/−}$
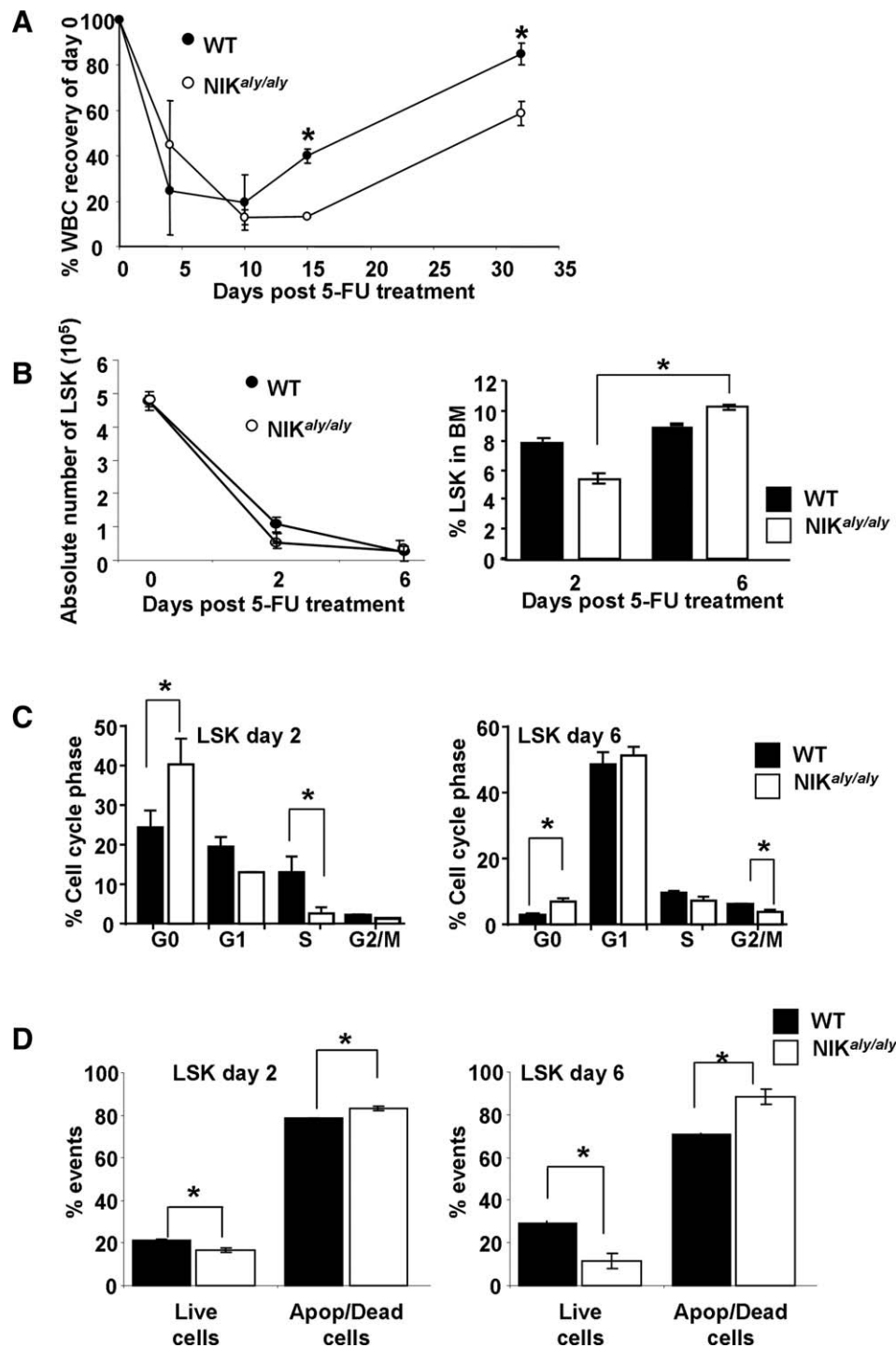
Figure 4. Delayed recovery of NIK$^{aly/aly}$ hematopoietic cells after 5-FU treatment. **(A)**: WBC counts after 5-FU treatment in P3B mice transplanted with total BM cells from NIK$^{aly/aly}$ or WT mice. The figure shows the percentage of WBC recovery normalized to pre-5FU treatment values ($n = 5$ per group). *, $p < .05$. **(B)**: Absolute number and percentage of LSK cells into BM of 5-FU treated mice. **(C)**: Cell cycle analysis. BM from NIK$^{aly/aly}$ or WT mice was analyzed after 2 days ($n = 3$ per group) and 6 days ($n = 3$ per group) of 5-FU treatment. **(D)**: Apoptosis analysis of LSK from treated mice, 2-day analysis ($n = 3$ per group) and 6-day analysis ($n = 3$ per group). Live cells were DAPI−AnnexinV−, apoptotic/dead cells were DAPI−AnnexinV + and DAPI+AnnexinV+. *, $p < .05$. Abbreviations: 5-FU, 5-fluorouracil; BM, bone marrow; LSK, Lin$^-$Sca1$^+$cKit$^+$; NIK, NFκB inducing kinase.

hematopoietic stem/progenitor cells was also confirmed by the recovery of PB leukocyte counts after 5-FU treatment (Fig. 6C). Finally, we further confirmed a delayed cell-cycle progression in response to cytokine stimulation in $NF\kappa B2^{-/-}$ cells, by Lin−

CFSE labeling (Supporting Information Fig. S5A). We observed a similar behavior between WT and $cRel^{-/-}$ cells, a complete delayed in NIK$^{aly/aly}$ cells, and a minor delay for NFκB2$^{-/-}$ cells in the dilution of CFSE (Supporting Information Fig. S5A).

Gene Expression Profile Analysis

To explore the consequences of the defective NIK$^{aly/aly}$ protein in alternative NFKB signaling in HSCs in homeostatic conditions, we investigated the gene expression profile of highly purified fresh LSK cells isolated from WT and NIK$^{aly/aly}$ mice using whole mouse genome oligo microarrays. The rational was to know the transcriptional basal state of HSC that could counterpart for its response to stress.

Data analysis revealed that 301 genes were differentially expressed (fold change ≥ 1.5 and p-value $< .05$) from which 148 were upregulated (49.2%) and 153 (50.8%) downregulated (Supporting Information Table S1). Based on these results, there was no clear evidence for NIK$^{aly/aly}$
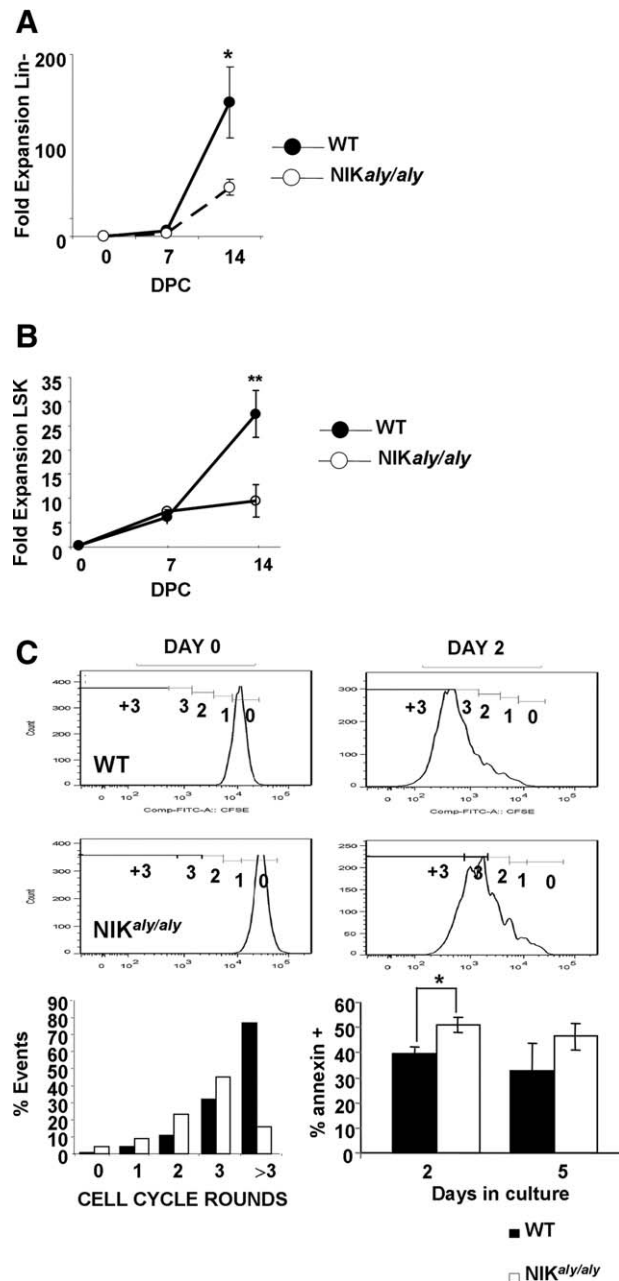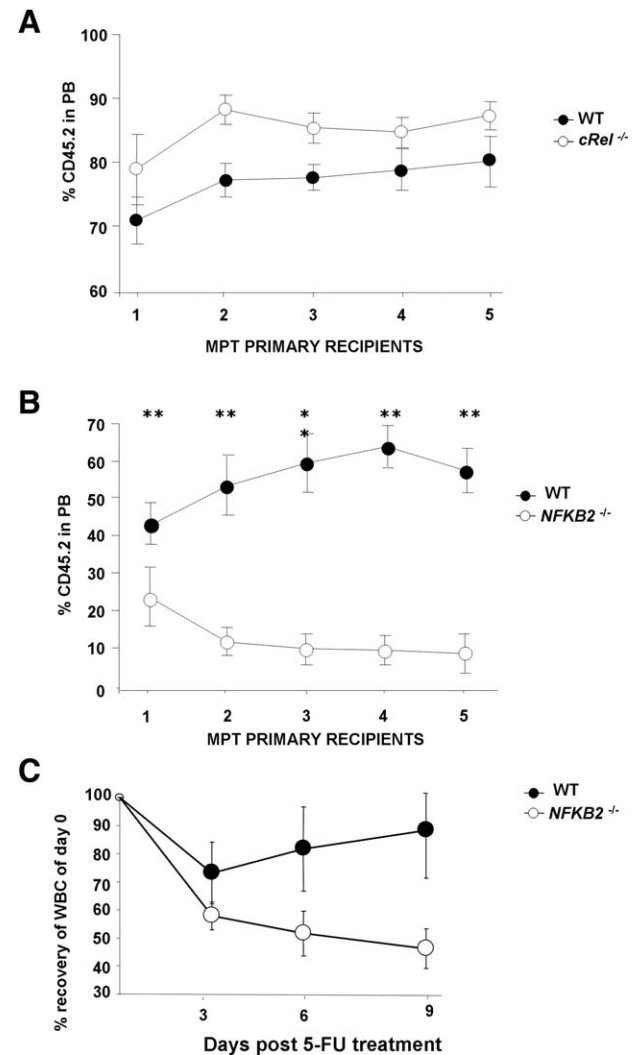
Figure 5. Expansion impairment of NIK$^{aly/aly}$ bone marrow (BM) cells in vitro due to proliferation defect and enhanced apoptosis. **(A)**: Liquid cultures of purified Lin− BM population from NIK$^{aly/aly}$ and WT mice, containing mSCF and hIL-11, were maintained during 14 days and total cell numbers and viability were analyzed weekly. *, $p < .05$. **(B)**: Liquid cultures of freshly sorted LSK population from NIK$^{aly/aly}$ and WT mice were maintained during 14 days and total cell numbers and viability were analyzed weekly. **, $p < .01$. **(C)**: Lin− BM was labeled with CSFE and cultured in presence of cytokines. CSFE dilution was analyzed several days after culture started. An estimation of rounds of cell division at day 2 is shown (down-left). Apoptotic cells (Annexin V+) in in vitro culture of NIK$^{aly/aly}$ and WT Lin− BM cells at days 2 and 5 after culture initiation (down-right). *, $p < .05$. Abbreviations: LSK, Lin−Sca1+cKit+; NIK, NFκB inducing kinase.

As shown with NIK$^{aly/aly}$ mice, basal hematopoiesis was normal in $NF\kappa B2^{-/-}$ and $cRel^{-/-}$ mice (Supporting Information Fig. S6).

Figure 6. Competitive repopulation assays to test NFκB2$^{-/-}$ and $cRel^{-/-}$ hematopoietic stem cells functionality. We performed competitive repopulation assays using mice knocked out for components of either pathway downstream NIK. CD45.2 kinetics in PB of recipient mice was represented for $cRel^{-/-}$ competition **(A)** and NFκB2$^{-/-}$ competition **(B)** ($n = 10$ per group). **, $p < .01$. **(C)**: WBC counts recovery after 5-FU treatment of NFκB2$^{-/-}$ chimera mice. Abbreviations: 5-FU, 5-fluorouracil; WBC, white blood cells.

Table 1. Regulated genes affecting different biological process

Biological process		NIK^aly/aly > WT	NIK^aly/aly < WT
Cell death	Positive regulation	TNFRSF11B (0.0151)	APOE (0.0089)
		TNFRSF11A	PCBP4
		PRKAA2	TXNIP
		UBE2K (0.0202)	LGALS1 (0.0274)
		TRIM13	P2RX7
			TNFSF12
			UNC5A (0.0185)
			STEAP3 (0.0106)
	Negative regulation	BEX2 (0.0121)	MET (0.0219)
		PARP16 (0.0095)	IL4 (0.0206)
		CHL1 (0.089)	CX3CR1
		GHR	GAS1
		MAPK8iP1(0.0099)	HDAC1 (0.0008)
		NKX3-2	
Cell proliferation	Positive regulation	PPARGC1A (0.0456)	MET (0.0219)
		SMARCD3	GDF9 (0.0252)
		LIPA (0.0436)	IL4 (0.0206)
		HDGFRP3 (0.070)	CSF1R (0.0026)
			MAPK1 (0.0408)
			GAS1
			HMGA2
			HDAC1 (0.0189)
	Negative regulation	PKP2 (0.0234)	APOE (0.0089)
		IRF6	TXNIP
		ROR2 (0.0027)	CEBPA
Cell cycle	Progression	BEX2 (0.0121)	PLCB1 (0.0308)
		CENPF	JUB (0.0051)
	Arrest	IRF6	PCBP4
			TXNIP
			E2F5
			ZC3H12D (0.054)
			GAS1
			PARP3 (0.0360)
			GAS2L3 (0.0460)
			STEAP3 (0.0106)
			MSH5 (0.0447)

Genes with no *p*-value resulted from analysis in which the fold-change was the only criterion.

being neither an overall transcriptional inductor nor a repressor.

We specifically focused on genes associated to cell cycle, cell death, and cell proliferation, key processes in the assays we have previously described. As shown in Table 1, genes with a known positive role in cell proliferation were mainly downregulated. However, genes promoting cell cycle arrest were also downregulated in NIK^aly/aly cells. In the same manner, genes with either positive or negative roles in cell death were similarly represented in number in the list of genes differentially regulated by NIK.

Among these 301 genes, up to 12 have been previously described as direct or indirect NFκB transcriptional targets (http://www.bu.edu/nf-kb/gene-resources/target-genes/). Interestingly, a search for putative binding sites on the regulatory regions of the 153 downregulated transcripts revealed that 146 (95.4%) of them beared at least one target site for any of the NFκB-transcription factor family members (Supporting Information Table S3).

We then challenged these altered genes in an IPA pathway analysis restricted to those pathways that had been previously implicated in HSC. Supporting Information Figure S7 shows a comprehensive list of statistically significant altered pathways. No classic pathways related to the HSC fate such as BMP/TGF-β, Wnt, or HOX transcription factors family among others were

found. Pathways such as Retinoic Acid Receptor (RAR) activation (*p*-value .0012), production of nitric oxide, and reactive oxygen species in macrophages (*p*-value .0012), involved in Reactive Oxigen Species (ROS) regulation, appeared as the most significantly altered ones. Regarding NIK deficiency, pathways related to the function of NIK in the immune system such as IL-12 signaling and production in macrophages (*p*-value .0081), role of osteoblasts, osteoclasts, and chondrocytes in rheumatoid arthritis (*p*-value .0234), and Lymphotoxin β receptor signaling (*p*-value .038) were also significantly altered.

DISCUSSION

In this study, we show that NIK has a role in the function of hematopoietic stem/progenitor cells under stress, but seems dispensable under homeostatic conditions. Of the various downstream pathways that NIK may activate [18, 49, 50], the NIK-p100/p52 pathway seems to be responsible for this function. NIK inactivation did not affect the numbers and proportions of stem/progenitor cell populations in BM in steady-state hematopoiesis, nor did it cause disturbances in mature cell numbers in PB (except for the reported defects in B cells) (Supporting Information Fig. S1). However, NIK-inactive HSCs had an impaired response to stressors such as supraphysiological levels of cytokines, myeloablative chemotherapy, or upon hematopoietic transplantation (Figs. 2, 4, 5).

The NIK^aly/aly mice used in this work bear a point mutation in the *Nik* gene [51], which renders the kinase unable to bind IKKα and P100 and so, p100 is not processed [52]. NIK^aly/aly mice, as well as NIK^−/− mice [27], have been used to study the role of NIK mainly in the immune system, since these animals have defects on lymphoid organogenesis and immune regulation [22, 23]. Some of these studies have shown both an intrinsic defect and also an important role of NIK in the stromal microenvironment of organs of the immune system (thymus, spleen, and lymph nodes), which negatively affected the function of NIK^aly/aly immune cells. Accordingly, marrow stromal cultures initiated with total BM cells from NIK^aly/aly mice have defects in supporting WT HSCs (our unpublished data). In this study, the transfer of NIK^aly/aly HSCs into the WT microenvironment of recipients allowed us to address the role of NIK in HSCs independently of its role on the BM environment. NIK^aly/aly HSCs engrafted in WT BM did not improve their functional capacities, underscoring an intrinsic role of NIK in HSCs, as shown in two different experiments. NIK^aly/aly HSCs placed on a WT BM did not respond as efficiently as control HSCs to 5-FU (Fig. 4) nor did it engraft as robustly in a competitive repopulation assay (Fig. 2A, 2E). In fact, 5 months after the first transplant, the numbers of LSK BM cells were lower in the mice recipients of NIK^aly/aly HSCs compared to those of mice transplanted with WT HSCs (Fig. 2D).

In vitro cultures showed that upon stimulation, NIK^aly/aly HSCs compartment, LSK, and the more heterogeneous Lin− population required a longer time to undergo rounds of cell divisions (Fig. 5B, left), plus they underwent apoptosis at higher rates than WT HSCs (Fig. 5B, right). The differences in apoptosis were more important early after the stimuli (Fig. 5B, right), in accordance with our previous results on activated T lymphocytes [21]. As a result of these combined

defects (early apoptosis and permanent impairment of proliferation), NIK$^{aly/aly}$ HSCs did not perform successfully in in vivo competitive repopulation transplants, nor regenerated hematopoiesis after 5-FU as fast as control WT HSCs.

Under 5-FU induced stress, the cycling status of LSK cells from NIK$^{aly/aly}$ was delayed compared to WT mice, as reflected by a higher percentage of cells in G0 at days 2 and 6 after treatment (Fig. 4C), and lower proportion of actively cycling cells. The role of NIK in apoptosis after stress was shown by the increased proportion of living cells after 5-FU treatment in the WT versus NIK$^{aly/aly}$ (Fig. 4D), 1.2-fold increase at day 2 and 2.5-fold at day 6. In accordance with in vitro cultures results, here we found that the day when LSK more actively proliferated (day 6, cell cycle analysis) was the moment when higher apoptosis was detected, likely due to higher sensitivity to activation induced cell death in NIK$^{aly/aly}$ LSK HSC. The similar total numbers of LSK at days 2 and 6 post-5-FU likely reflected a balance between the higher apoptosis of activated cells and the higher proportions of quiescent LSK HSCs. An additional consequence of the delayed cell cycle progression of the NIK$^{aly/aly}$ LSK cell population was their kinetics in BM after 5-FU. While day 2 values of LSK from NIK$^{aly/aly}$ were comparable to those at steady-state (compare to Fig. 1B), a faster increase from basal levels was detected in the LSK proportions of WT mice. This increase was maintained at day 6 among LSK WT but proportions of NIK$^{aly/aly}$ LSK almost doubled at day 6, probably reflecting the higher percentages of quiescent LSK at day 2. It is well known that NFκB is involved in survival/antiapoptosis through proteins such as FLICE inhibitory protein, cIAP, surviving, Bcl-2, and Bcl-XL, and regulates the expression of genes related to cell growth, proliferation, differentiation, immune response, and inflammation [53]. We and others previously showed that NIK-deficient T lymphocytes were not able to generate GVHD because of high rates of apoptosis [21, 25]. Jin et al. described that NIK$^{-/-}$ mice (and NIK$^{-/-}$ T cell-transferred Rag2$^{-/-}$ mice) were resistant to EAE induction by Myelin Oligodendrocyte Glycoproteine (MOG) immunization, mainly because their T lymphocytes have limited proliferative capacity and Th17 differentiation [26]. Our results suggest that the loss of NIK negatively affects HSCs whenever they need to deal with stress. The fact that we found the major disturbances in HSCs function after stress and not under physiological conditions may suggest that the intensity of the signal should be important, as stress signals for HSCs during steady-state hematopoiesis should be milder than those during during hematopoietic reconstitution, that is, BM transplantation or administration of 5-FU. The absence of a fully functional NIK protein resulted in a delay in the duration of the cell cycle (Fig. 4C, 5B, left) and in apoptosis (Fig. 4D, 5B, right) when coping with stress. We cannot rule out the possibility that NIK$^{aly/aly}$ HSCs may accumulate defects during steady state that only manifest under protracted stresses.

We found comparable defects when using NIK$^{aly/aly}$ HSCs and NFκb2$^{-/-}$ HSCs (Fig. 6B). These results underscore the role of the NIK-p100/p52 activation pathway in HSCs. There are two main pathways for NFκB activation. Canonical or classic pathway activation is rapid and transient and acts independently of protein synthesis. Noncanonical or alternative pathway is slower but persistent, and depends on de novo protein synthesis [50, 54, 55]. Noncanonical pathway regulates

lymphoid organogenesis, B-cell survival and maturation, dendritic cell activation, and bone metabolism. Little is known about the role of the alternative pathway in HSC function. Zhao et al. [37] analyzed the HSC function in NFκb2$^{-/-}$/Relb$^{-/-}$ double Knockout (KO), in which the alternative NFκB pathway is not functional. Similar to what we show here for the NIK$^{aly/aly}$ and the NFκb2$^{-/-}$ mice, Zhao et al. described a defect in the repopulation ability of double NFκb2$^{-/-}$/Relb$^{-/-}$ HSCs in competitive and noncompetitive assays. However, these authors observed an increased frequency of LSK population and a decreased of CD150+CD48−LSK or CD34−CD135−LSK in steady state in the double KO mice. They also observed a high proportion of proliferative cells in LSK cells and decreased in apoptotic cells. Some of the HSC defects described in the double KO model improved when HSCs were transferred into a wild-type marrow environment. In our models, NIK$^{aly/aly}$ mice did not present significant differences in HSC subpopulations nor in the cell cycle status in basal conditions (Fig. 1), and the transfer into a WT BM did not recover the functional capacities of HSCs (Figs. 2, 4). The differences found between our experiments and those of Zhao et al. may be related to the different KO molecules the NIK protein should be active in the double KO model, suggesting that in HSCs, NIK may also signal through mediators other than p100-p52-Relb.

The number of NIK regulated genes in our gene expression analysis was low if we compare it with published data (Supporting Information Fig. S7 and Supporting Information Table S1). One possible explanation is that NIK and genes of the alternative NFκB pathway are expressed at higher levels in lymphoid tissues compared to LSK HSCs. However, some of the genes identified in our study have already been found in other cellular systems, validating the significance of our work (Supporting Information Table S2) [56–59]. The results from the array study supported the findings obtained in the functional assays shown in this work. The downregulation in the expression levels of genes that have a positive role in cell proliferation combined with the downregulation in the expression levels of genes involved in cell cycle arrest (Table 1) in resting NIK$^{aly/aly}$ HSCs suggest that these stem cells are not impaired for activating the cell cycle machinery but they are not fully equipped to actively respond to proliferative signals. In accordance with this, we did not find any significant difference in the distribution of HSCs along the different phases of the cell cycle in steady-state (Fig. 1C) but did find a delay on CFSE dilution in in vitro experiments. Regarding the different levels of apoptosis found in Figure 5B, basal expression levels of apoptosis-related genes were not affected by the NIK$^{aly/aly}$ mutation. This suggests that apoptosis is related to activation of HSC in these cells, as we have previously shown during T-cell activation [21]. The results of our analysis revealed a potential role for pathways (in Supporting Information Fig. S7) already related with HSC survival, that is, ROS metabolism [9].

Cells from the immune system and from nonhematopoietic tissues produce cytokines during infections or stress that activate HSC through innate immune signaling pathways. Conversely, HSC can respond to Toll-Like receptors (TLR) stimulation [60, 61] leading to an increased myeloid cell production and NFκB has been implicated in this response. It is temptative to speculate that a deficit in NFκB signaling in this

context (as shown in our models) would result in an impaired response to the stress. It is interesting to note that molecules related with TLR signaling came up in our gene expression analysis, such as *Tlr6, Irf8, Il4*, some TNF receptors (*Tnfrsf11b*), or TGF-β signaling (*Smad5*), all of them genes that regulate proliferation and differentiation of HSC.

CONCLUSIONS

In summary, our results suggest that NIK and the noncanonical NFκB pathway are needed for HSCs to respond to stressful conditions, while it could be dispensable during steady-state hematopoiesis. The inactivation of this kinase would be detrimental for the hematopoietic system in vivo, a strategy we initially contemplated in the allogeneic setting [21].

AUTHOR CONTRIBUTIONS

Á.G.-M.: conception and design, collection and/or assembly of data, data analysis and interpretation, manuscript writing, and final approval of manuscript; L.F.: conception and design, collection and/or assembly of data, and final approval of manuscript; S.B., G.J.M., and R.S.: collection and/or assembly of data and final approval of manuscript; C.S.-V.: final approval of manuscript; J.C.S.: provision of study material or patients, collection and/or assembly of data, and final approval of manuscript; H.-C.L., R.S., and L.M.: provision of study material or patients and final approval of manuscript; M.F.: conception and design, financial support, provision of study material or patients, data analysis and interpretation, and final approval of manuscript; M.R.: conception and design, financial support, data analysis and interpretation, manuscript writing, and final approval of manuscript.

DISCLOSURE OF POTENTIAL CONFLICTS OF INTEREST

The authors indicate no potential conflicts of interest.

REFERENCES

1 Kimura S, Roberts AW, Metcalf D et al. Hematopoietic stem cell deficiencies in mice lacking c-Mpl, the receptor for thrombopoietin. Proc Natl Acad Sci USA 1998;95:1195–1200.

2 Metcalf D. Lineage commitment and maturation in hematopoietic cells: The case for extrinsic regulation. Blood 1998;92:345–347; discussion 352.

3 Klump H, Schiedlmeier B, Baum C. Control of self-renewal and differentiation of hematopoietic stem cells: HOXB4 on the threshold. Ann N Y Acad Sci 2005;1044:6–15.

4 Park IK, Qian D, Kiel M et al. Bmi-1 is required for maintenance of adult self-renewing haematopoietic stem cells. Nature 2003;423:302–305.

5 Cheng T, Rodrigues N, Dombkowski D et al. Stem cell repopulation efficiency but not pool size is governed by p27(kip1). Nat Med 2000;6:1235–1240.

6 Cheng T, Rodrigues N, Shen H et al. Hematopoietic stem cell quiescence maintained by p21cip1/waf1. Science 2000;287:1804–1808.

7 Yuan Y, Shen H, Franklin DS et al. In vivo self-renewing divisions of haematopoietic stem cells are increased in the absence of the early G1-phase inhibitor, p18INK4C. Nat Cell Biol 2004;6:436–442.

8 Ito K, Hirao A, Arai F et al. Regulation of oxidative stress by ATM is required for self-renewal of haematopoietic stem cells. Nature 2004;431:997–1002.

9 Ito K, Hirao A, Arai F et al. Reactive oxygen species act through p38 MAPK to limit the lifespan of hematopoietic stem cells. Nat Med 2006;12:446–451.

10 Tothova Z, Kollipara R, Huntly BJ et al. FoxOs are critical mediators of hematopoietic stem cell resistance to physiologic oxidative stress. Cell 2007;128:325–339.

11 Morrison SJ, Wright DE, Weissman IL. Cyclophosphamide/granulocyte colony-stimulating factor induces hematopoietic stem cells to proliferate prior to mobilization. Proc Natl Acad Sci USA 1997;94:1908–1913.

12 Wright DE, Cheshier SH, Wagers AJ et al. Cyclophosphamide/granulocyte colony-stimulating factor causes selective mobilization of bone marrow hematopoietic stem cells into the blood after M phase of the cell cycle. Blood 2001;97:2278–2285.

13 Aggarwal BB, Takada Y, Shishodia S et al. Nuclear transcription factor NF-kappa B: Role in biology and medicine. Indian J Exp Biol 2004;42:341–353.

14 Hayden MS, Ghosh S. Shared principles in NF-kappaB signaling. Cell 2008;132:344–362.

15 Vallabhapurapu S, Karin M. Regulation and function of NF-kappaB transcription factors in the immune system. Annu Rev Immunol 2009;27:693–733.

16 Ghosh S, May MJ, Kopp EB. NF-kappa B and Rel proteins: Evolutionarily conserved mediators of immune responses. Annu Rev Immunol 1998;16:225–260.

17 Malinin NL, Boldin MP, Kovalenko AV et al. MAP3K-related kinase involved in NF-kappaB induction by TNF, CD95 and IL-1. Nature 1997;385:540–544.

18 Xiao G, Harhaj EW, Sun SC. NF-kappaB-inducing kinase regulates the processing of NF-kappaB2 p100. Mol Cell 2001;7:401–409.

19 Senftleben U, Cao Y, Xiao G et al. Activation by IKKalpha of a second, evolutionary conserved, NF-kappa B signaling pathway. Science 2001;293:1495–1499.

20 Xiao G, Fong A, Sun SC. Induction of p100 processing by NF-kappaB-inducing kinase involves docking IkappaB kinase alpha (IKKalpha) to p100 and IKKalpha-mediated phosphorylation. J Biol Chem 2004;279:30099–30105.

21 Sanchez-Valdepenas C, Casanova L, Colmenero I et al. Nuclear factor-kappaB inducing kinase is required for graft-versus-host disease. Haematologica 2010;95:2111–2118.

22 Miyawaki S, Nakamura Y, Suzuka H et al. A new mutation, aly, that induces a generalized lack of lymph nodes accompanied by immunodeficiency in mice. Eur J Immunol 1994;24:429–434.

23 Shinkura R, Matsuda F, Sakiyama T et al. Defects of somatic hypermutation and class switching in alymphoplasia (aly) mutant mice. Int Immunol 1996;8:1067–1075.

24 Yamada T, Mitani T, Yorita K et al. Abnormal immune function of hemopoietic cells from alymphoplasia (aly) mice, a natural strain with mutant NF-kappa B-inducing kinase. J Immunol 2000;165:804–812.

25 Murray SE, Polesso F, Rowe AM et al. NF-kappaB-inducing kinase plays an essential T cell-intrinsic role in graft-versus-host disease and lethal autoimmunity in mice. J Clin Invest 2011;121:4775–4786.

26 Jin W, Zhou XF, Yu J et al. Regulation of Th17 cell differentiation and EAE induction by MAP3K NIK. Blood 2009;113:6603–6610.

27 Aya K, Alhawagri M, Hagen-Stapleton A et al. NF-(kappa)B-inducing kinase controls lymphocyte and osteoclast activities in inflammatory arthritis. J Clin Invest 2005;115:1848–1854.

28 Nonaka M, Horie R, Itoh K et al. Aberrant NF-kappaB2/p52 expression in Hodgkin/Reed-Sternberg cells and CD30-transformed

rat fibroblasts. Oncogene 2005;24:3976–3986.

29 Saitoh Y, Yamamoto N, Dewan MZ et al. Overexpressed NF-kappaB-inducing kinase contributes to the tumorigenesis of adult T-cell leukemia and Hodgkin Reed-Sternberg cells. Blood 2008;111:5118–5129.

30 Xiao G, Cvijic ME, Fong A et al. Retroviral oncoprotein Tax induces processing of NF-kappaB2/p100 in T cells: Evidence for the involvement of IKKalpha. EMBO J 2001;20:6805–6815.

31 Yamagishi M, Nakano K, Miyake A et al. Polycomb-mediated loss of miR-31 activates NIK-dependent NF-kappaB pathway in adult T cell leukemia and other cancers. Cancer Cell 2012;21:121–135.

32 Annunziata CM, Davis RE, Demchenko Y et al. Frequent engagement of the classical and alternative NF-kappaB pathways by diverse genetic abnormalities in multiple myeloma. Cancer Cell 2007;12:115–130.

33 Dejardin E, Bonizzi G, Bellahcene A et al. Highly-expressed p100/p52 (NFKB2) sequesters other NF-kappa B-related proteins in the cytoplasm of human breast cancer cells. Oncogene 1995;11:1835–1841.

34 Nishina T, Yamaguchi N, Gohda J et al. NIK is involved in constitutive activation of the alternative NF-kappaB pathway and proliferation of pancreatic cancer cells. Biochem Biophys Res Commun 2009;388:96–101.

35 Saitoh Y, Martinez Bruyn VJ, Uota S et al. Overexpression of NF-kappaB inducing kinase underlies constitutive NF-kappaB activation in lung cancer cells. Lung Cancer 2010;70:263–270.

36 Wharry CE, Haines KM, Carroll RG et al. Constitutive non-canonical NFkappaB signaling in pancreatic cancer cells. Cancer Biol Ther 2009;8:1567–1576.

37 Zhao C, Xiu Y, Ashton J et al. Noncanonical NF-kappaB signaling regulates hematopoietic stem cell self-renewal and microenvironment interactions. Stem Cells 2012;30:709–718.

38 Paxian S, Merkle H, Riemann M et al. Abnormal organogenesis of Peyer's patches in mice deficient for NF-kappaB1, NF-kappaB2, and Bcl-3. Gastroenterology 2002;122:1853–1868.

39 Liou HC, Jin Z, Tumang J et al. c-Rel is crucial for lymphocyte proliferation but dispensable for T cell effector function. Int Immunol 1999;11:361–371.

40 Medvinsky AL, Gan OI, Semenova ML et al. Development of day-8 colony-forming unit-spleen hematopoietic progenitors during early murine embryogenesis: Spatial and temporal mapping. Blood 1996;87:557–566.

41 Albella B, Segovia JC, Guenechea G et al. Preserved long-term repopulation and differentiation properties of hematopoietic grafts subjected to ex vivo expansion with stem cell factor and interleukin 11. Transplantation 1999;67:1348–1357.

42 Spangrude GJ, Heimfeld S, Weissman IL. Purification and characterization of mouse hematopoietic stem cells. Science 1988;241:58–62.

43 Uchida N, Aguila HL, Fleming WH et al. Rapid and sustained hematopoietic recovery in lethally irradiated mice transplanted with purified Thy-1.1lo Lin-Sca-1 + hematopoietic stem cells. Blood 1994;83:3758–3779.

44 Lu R, Neff NF, Quake SR et al. Tracking single hematopoietic stem cells in vivo using high-throughput sequencing in conjunction with viral genetic barcoding. Nat Biotechnol 2011;29:928–933.

45 Forsberg EC, Prohaska SS, Katzman S et al. Differential expression of novel potential regulators in hematopoietic stem cells. PLoS Genet 2005;1:e28.

46 Kiel MJ, Yilmaz OH, Iwashita T et al. SLAM family receptors distinguish hematopoietic stem and progenitor cells and reveal endothelial niches for stem cells. Cell 2005;121:1109–1121.

47 Okada S, Nakauchi H, Nagayoshi K et al. In vivo and in vitro stem cell function of c-kit- and Sca-1-positive murine hematopoietic cells. Blood 1992;80:3044–3050.

48 Chen Y, Ma X, Zhang M et al. Gadd45a regulates hematopoietic stem cell stress responses in mice. Blood 2014;123:851–862.

49 Sanchez-Valdepenas C, Martin AG, Ramakrishnan P et al. NF-kappaB-inducing kinase is involved in the activation of the CD28 responsive element through phosphorylation of c-Rel and regulation of its transactivating activity. J Immunol 2006;176:4666–4674.

50 Sun SC. Non-canonical NF-kappaB signaling pathway. Cell Res 2011;21:71–85.

51 Shinkura R, Kitada K, Matsuda F et al. Alymphoplasia is caused by a point mutation in the mouse gene encoding Nf-kappa b-inducing kinase. Nat Genet 1999;22:74–77.

52 Luftig MA, Cahir-McFarland E, Mosialos G et al. Effects of the NIK aly mutation on NF-kappaB activation by the Epstein-Barr virus latent infection membrane protein, lymphotoxin beta receptor, and CD40. J Biol Chem 2001;276:14602–14606.

53 Aggarwal BB. Nuclear factor-kappaB: The enemy within. Cancer Cell 2004;6:203–208.

54 Claudio E, Brown K, Park S et al. BAFF-induced NEMO-independent processing of NF-kappa B2 in maturing B cells. Nat Immunol 2002;3:958–965.

55 Liang C, Zhang M, Sun SC. beta-TrCP binding and processing of NF-kappaB2/p100 involve its phosphorylation at serines 866 and 870. Cell Signal 2006;18:1309–1317.

56 Lovas A, Radke D, Albrecht D et al. Differential RelA- and RelB-dependent gene transcription in LTbetaR-stimulated mouse embryonic fibroblasts. BMC Genomics 2008;9:606.

57 Lovas A, Weidemann A, Albrecht D et al. p100 Deficiency is insufficient for full activation of the alternative NF-kappaB pathway: TNF cooperates with p52-RelB in target gene transcription. PLoS One 2012;7:e42741.

58 Bunting K, Rao S, Hardy K et al. Genome-wide analysis of gene expression in T cells to identify targets of the NF-kappa B transcription factor c-Rel. J Immunol 2007;178:7097–7109.

59 Pahl HL. Activators and target genes of Rel/NF-kappaB transcription factors. Oncogene 1999;18:6853–6866.

60 Nagai Y, Garrett KP, Ohta S et al. Toll-like receptors on hematopoietic progenitor cells stimulate innate immune system replenishment. Immunity 2006;24:801–812.

61 Megias J, Yanez A, Moriano S et al. Direct Toll-like receptor-mediated stimulation of hematopoietic stem and progenitor cells occurs in vivo and promotes differentiation toward macrophages. Stem Cells 2012;30:1486–1495.

See www.StemCells.com for supporting information available online.